

Synthesis of Co(II)-Imidazolate Framework from Anionic Linker Precursor: Gas-Sorption and Magnetic Properties

Suwendu Sekhar Mondal,^a Asamanjoy Bhunia,^b Serhiy Demeshko,^c Alexandra Kelling,^a Uwe Schilde,^a Christoph Janiak,^b and Hans-Jürgen Holdt*^a

^a *Institut für Chemie, Anorganische Chemie, Universität Potsdam, Karl-Liebknecht-Straße 24-25, 14476 Potsdam, Germany.*

Fax: +49 331-977-5055; Tel: +39 331-977-5180; E-mail: holdt@uni-potsdam.de

^b *Institut für Anorganische Chemie und Strukturchemie, Heinrich-Heine-Universität Düsseldorf, 40204 Düsseldorf, Germany*

^c *Institut für Anorganische Chemie, Georg-August-Universität Göttingen, Tammannstraße 4, 37077 Göttingen, Germany*

Supporting Information
(15 pages)

CONTENTS

| | |
|--|-------------|
| 1 General Remarks | S-1 |
| 2 Syntheses | S-2 |
| 3 SEM Images | S-3 |
| 4 DSC Curves | S-3 |
| 5 IR Spectra | S-4 |
| 6 NMR Spectra | S-6 |
| 7 Powder X-ray Diffraction Data | S-7 |
| 7 Single Crystal X-ray Diffraction Data | S-9 |
| 8 Thermogravimetric Analysis Data | S-11 |
| 9 Gas-sorption | S-12 |
| 10 Magnetic Measurement | S-14 |
| References | S-15 |

General Remarks

Elemental analysis (C, H, N) was performed on Elementar Vario EL elemental analyzer.

^1H and ^{13}C NMR spectra (for ionic liquid) were performed on Bruker Advanced 500 spectrometer using the residual protons of the solvent as an internal standard.

The ESI-MS was recorded using a Micromass Q-TOF_{micro} mass spectrometer in positive electrospray mode. Scanning Electron Micrographs (SEM) image of IFP-5 was taken by Phenom from FEICO. Melting point, crystallization and glass transition temperatures of the ionic liquid were determined by differential scanning calorimetry using Mettler Toledo DSC 822e. All reagents and solvents were used as purchased from commercial suppliers (Sigma-Aldrich, Fluka, Alfa Aesar, and others) without further purification, if not stated otherwise.

Syntheses

Ionic liquid synthesis

The linker 4,5-dicyano-2-methylimidazole (1)¹ was synthesized according to previous report, whereas the ionic liquid was synthesized according to published procedure.² Anhydrous potassium carbonate (1.33 g, 9.6 mmol) was added to a solution of 4,5-dicyano-2-methylimidazole (0.85 g, 6.4 mmol) in acetone (50 mL) at room temperature. The reaction mixture was stirred for 6–7 h. Then dichloromethane (50 mL) solution of corresponding tetraethylammonium chloride (1.06 g, 6.4 mmol) was added for the synthesis of ionic liquid (IL1) and reaction mixture was stirred for 3–4 h. The mixture was filtered and concentrated under vacuum. The product was extracted with acetone, the extract was filtered, and resultant solvent was dried to produce ionic liquid.

Tetraethylammonium 4,5-dicyano-2-methylimidazolate (IL1):

^1H NMR (CDCl_3): δ = 1.23–1.29 (m, 12H), 2.29 (s, 3H), 3.19 (quart., J = 7.3 Hz, 8H) ppm; ^{13}C NMR (CDCl_3): δ = 7.5, 16.8, 52.7, 116.9, 117.9, 157.5 ppm; ESI-MS: m/z (%): 130 (100) for cation, 131 (100) for anion; elemental analysis calcd., (%) for $\text{C}_{14}\text{H}_{23}\text{N}_5$ (261.4): C 64.34, H 8.87, N 26.80; found: C 64.19, H 9.10, N 27.08; $T_{\text{s-s}}$ = 55.0 °C, 74.2 °C, T_{m} = 98.9 °C.

Synthesis of IFP-5: In a sealed tube (type A, company: Ace), tetraethylammonium 4,5-dicyano-2-methylimidazolate (0.07 g, 0.26 mmol) and $\text{Co}(\text{NO}_3)_2 \cdot 6\text{H}_2\text{O}$ (0.08 g, 0.26 mmol) were dissolved in DMF (3 mL) in 6 mL DMF. The tube was closed and the mixture was heated at 130 °C for 48 hours. After cooling the mixture to room temperature, fine purple micro crystals were obtained by filtration and dried in air. Yield: ~ 55 % based on ionic liquid precursor; elemental analysis of activated IFP-5: $\text{C}_6\text{H}_6\text{CoN}_4\text{O}_2$; Calcd., C 32.02, H 2.69, N 24.89, Found: C 32.43, H 2.35, N 25.11; IR (KBr pellet): ν_{max} = 3328 (m), 3107 (m), 1658 (s),

1546 (vs), 1508 (m), 1477 (m), 1438 (m), 1284 (m), 1267 (m), 1227 (m), 1113 (m), 823 (m), 738 cm^{-1} (m).

SEM image of IFP-5

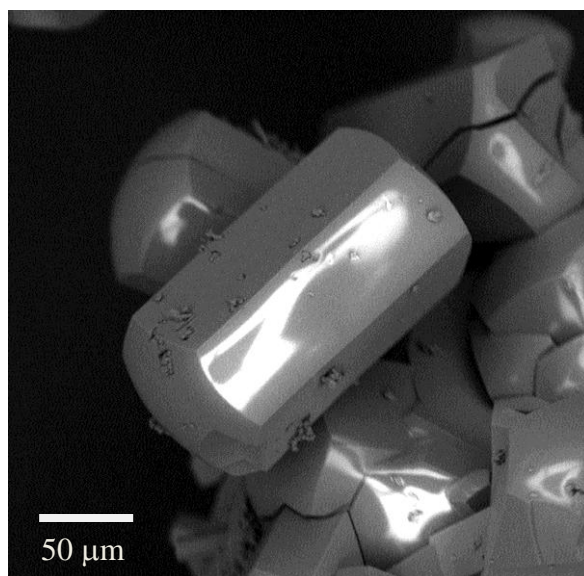


Fig. S1 Scanning electron micrograph of IFP-5.

DSC Curve of ionic liquid

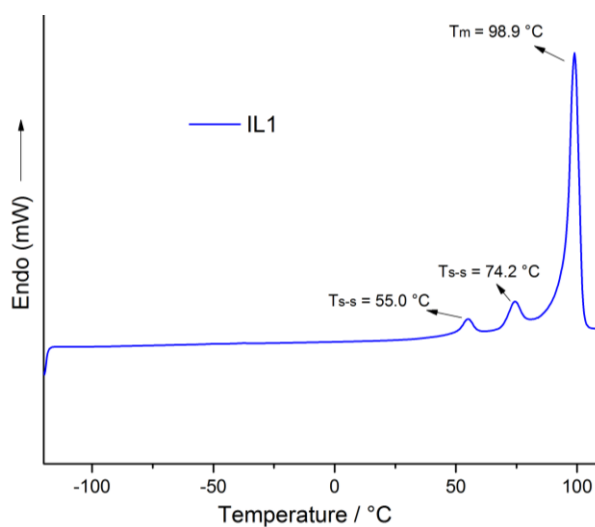
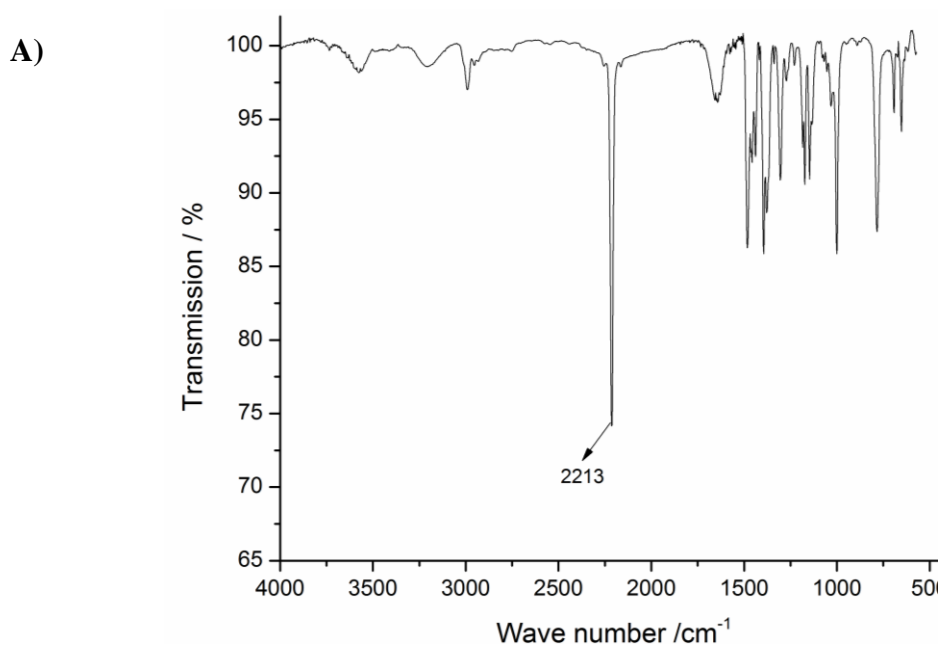


Fig. S2 Representative DSC trace recorded at a heating rate of 10 °C /min in the second heating cycle. T_{s-s} and T_m represent the solid-solid transition and melting temperatures, respectively.

IR spectra

IR spectra were recorded on FT-IR Nexus from Thermo Nicolet in the region of 4000 – 400 cm^{-1} using KBr pellets as basis.

The degree of in situ hydrolysis of the cyano groups of 4,5-dicyano-2-methylimidazolate anion into the corresponding imidazolate-4-amide-5-imide linker (L1) was studied with infrared (IR) spectroscopy. The IR-spectra of IFP-5 manifested no stretching bands related to $\text{C}\equiv\text{N}$ in the region of 2205–2225 cm^{-1} . Instead, new typical bands for amide and imide groups were observed at around 1580 cm^{-1} and 1660 cm^{-1} . Among other prominent IR changes, those associated with N–H resonances were noticeable. Centered at 3325 cm^{-1} , a broad amide-imide N–H band with considerable fine structure was noted.



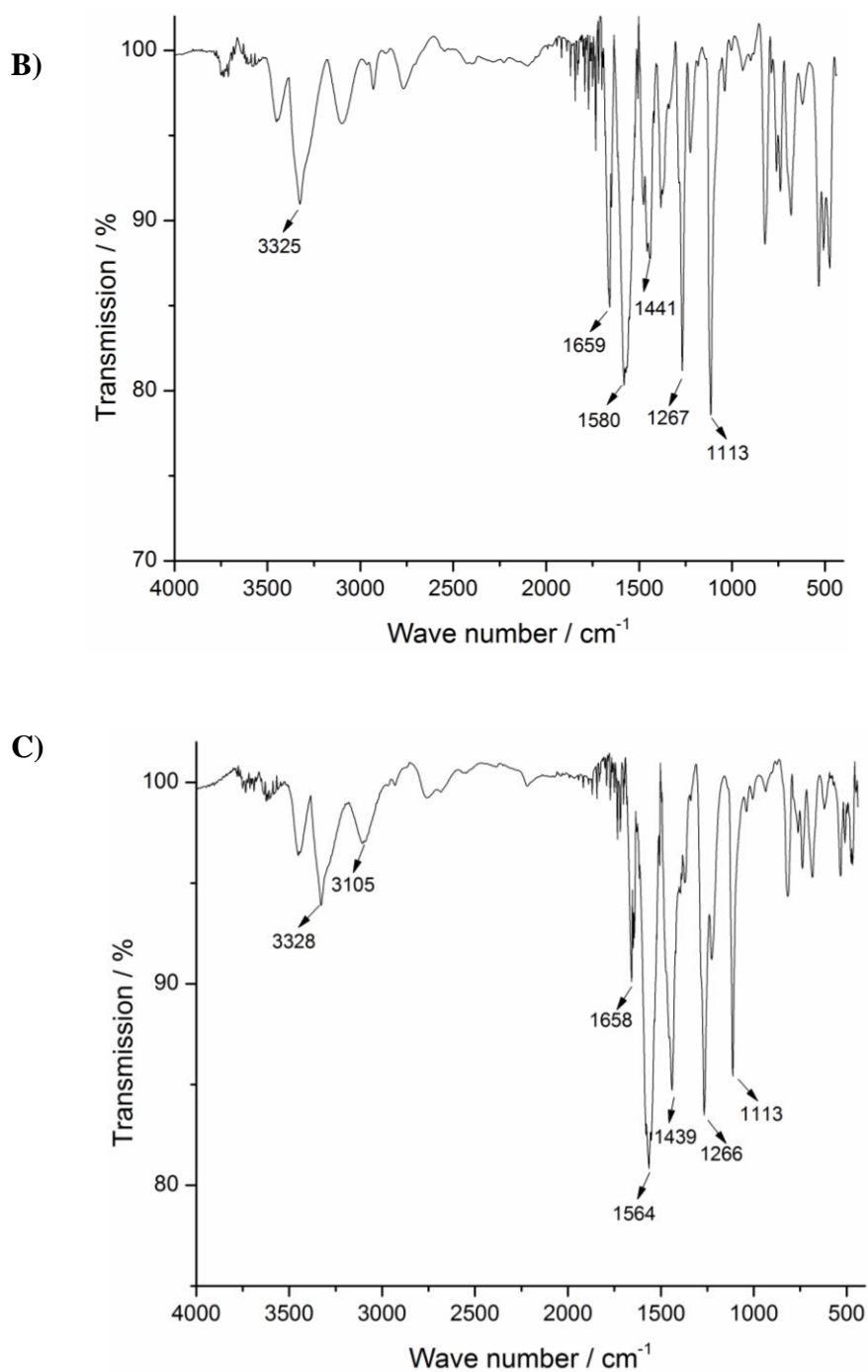


Fig. S3. IR-spectra of: **A)** Tetraethylammonium 4,5-dicyano-2-methylimidazolate (IL1); **B)** IFP-5 as-synthesized; **C)** IFP-5 activated at 200°C and 10^{-3} mbar for 24 h.

NMR spectra

NMR spectra of Ionic liquid

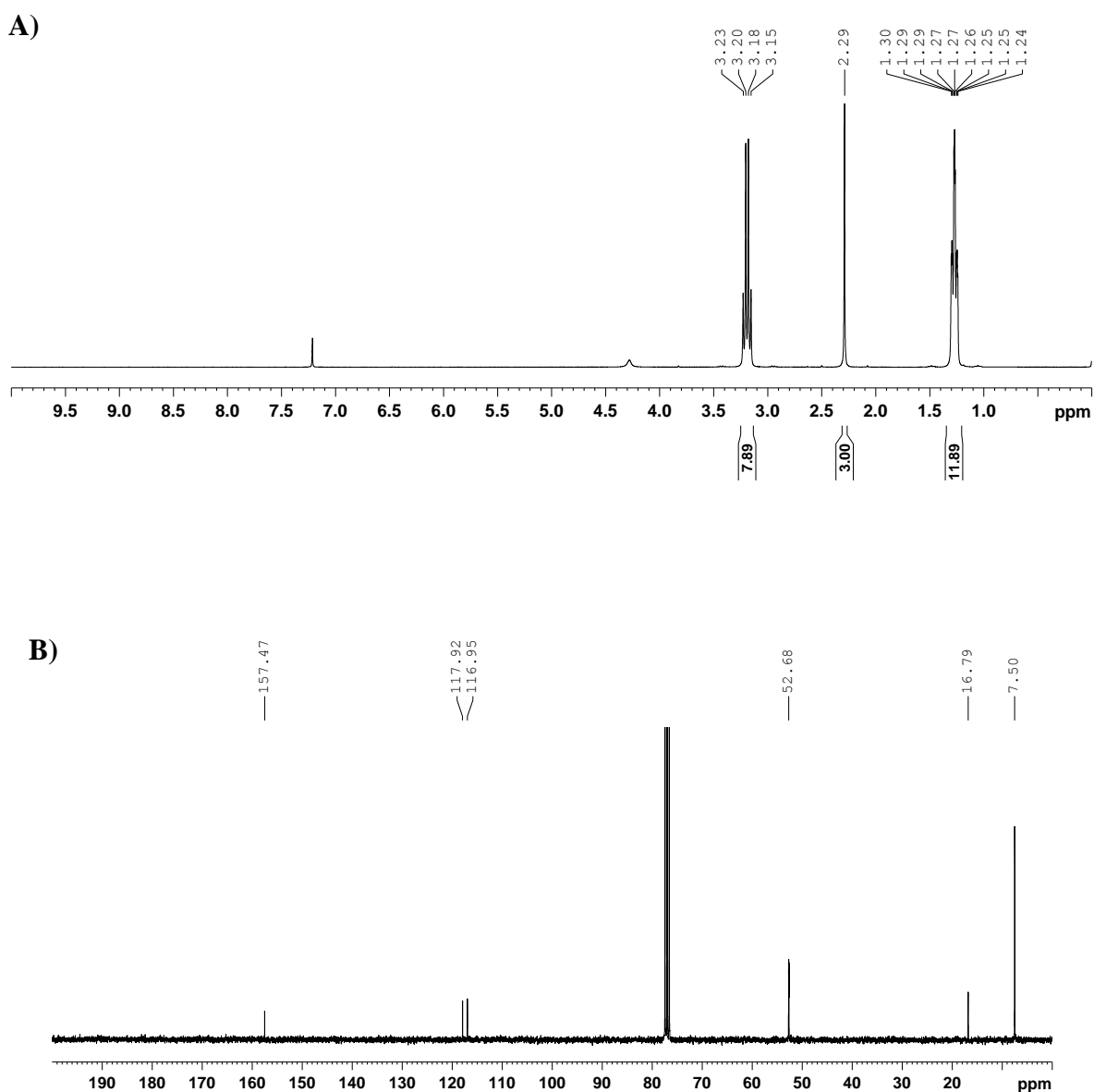


Fig. S4. ^1H - **A)** and ^{13}C - **B)** NMR spectra of ionic liquid, IL1.

Powder X-ray-diffraction patterns

Powder X-ray diffraction (PXRD) patterns of IFP-5 were measured on a Siemens Diffractometer D5005 in Bragg-Brentano reflection geometry. The diffractometer was equipped with a copper tube, a scintillation counter, automatic incident- and diffracted-beam soler slits and a graphite secondary monochromator. The generator was set to 40 kV and 40 mA. All measurements were performed with sample rotation. Data were collected digitally from 3° to 70° 2θ using a step size of 0.02° 2θ and a count time of 4 seconds per step. The simulated powder patterns for IFP-5 were calculated using single-crystal X-ray diffraction data and processed by the free Mercury v1.4.2 program provided by the Cambridge Crystallographic Data Centre.

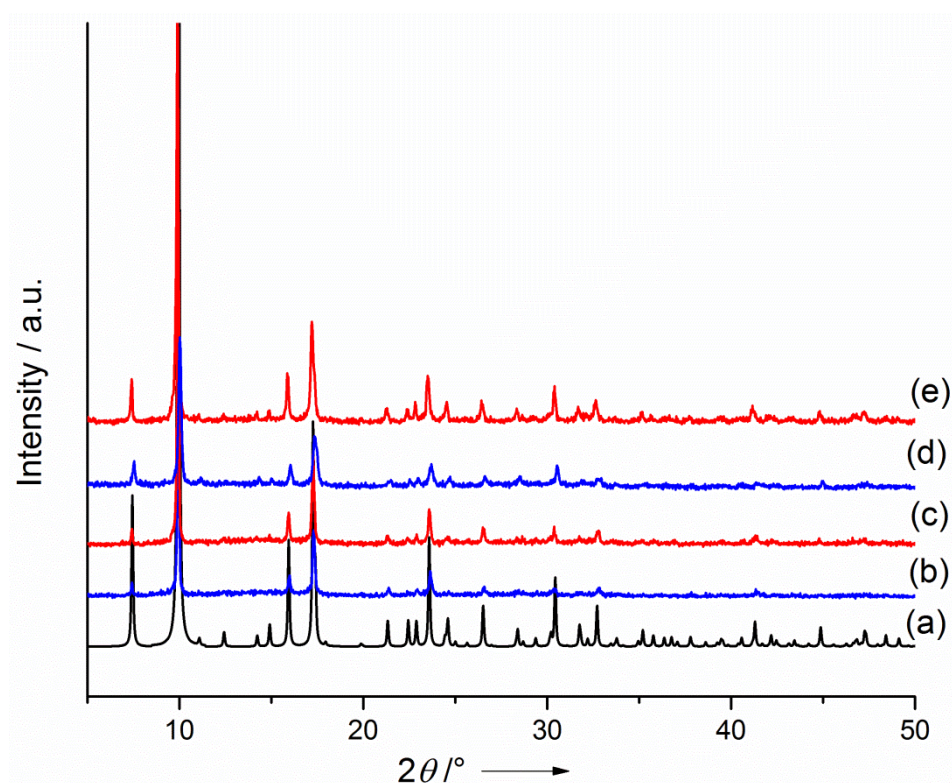


Fig. S5. Powder X-ray diffraction patterns of IFP-5 a) simulated, using ionic liquid IL1 precursor; b) as-synthesized from 2 and c) activated; d) using ionic liquid IL1 precursor as-synthesized and e) activated.

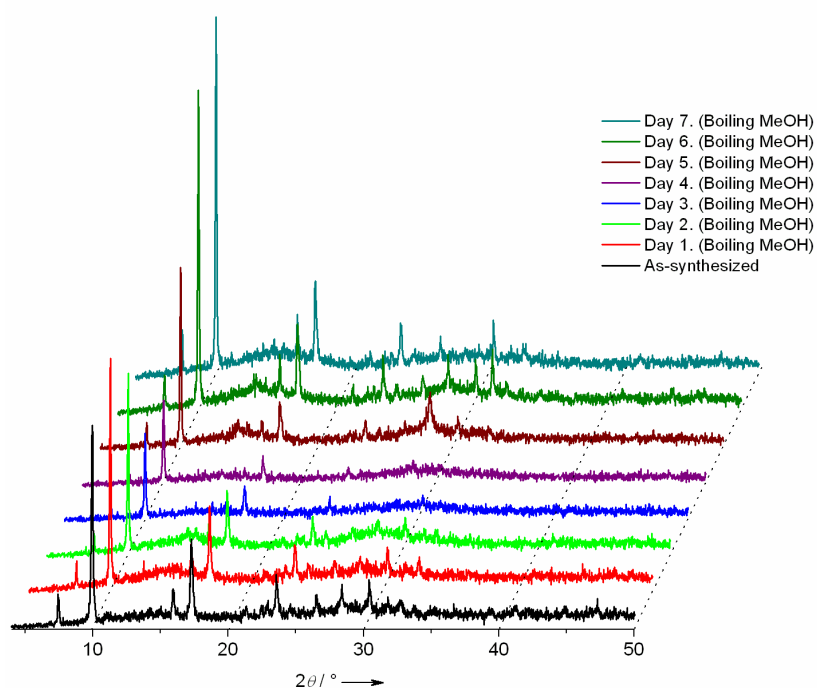


Fig. S6. Powder X-ray diffraction profiles of IFP-5 collected during stability tests in refluxing methanol.

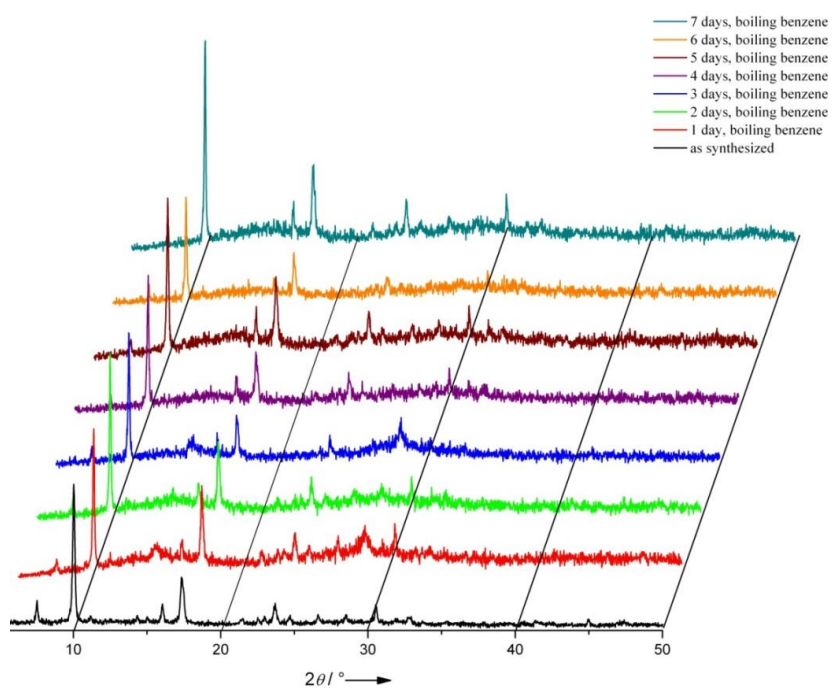


Fig. S7. Powder X-ray diffraction profiles of IFP-5 collected during stability tests in refluxing benzene.

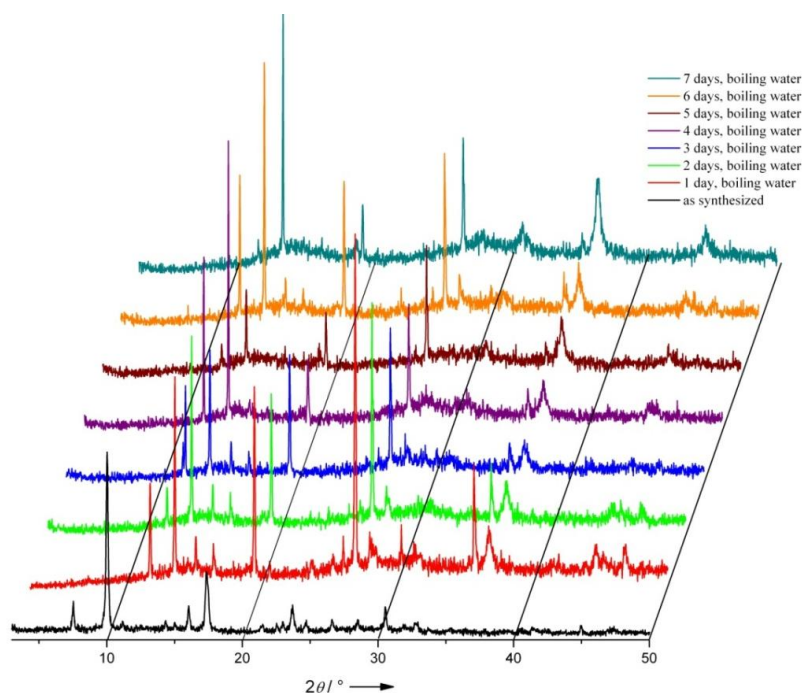


Fig. S8. Powder X-ray diffraction profiles of IFP-5 collected during stability tests in refluxing water.

Single crystal X-ray structure determination

The crystal was embedded in perfluoropolyalkylether oil and mounted on a glass fibre. Intensity data were collected at 210 K using a STOE Imaging Plate Diffraction System IPDS-2 with graphite monochromatized $\text{MoK}\alpha$ radiation ($\lambda = 0.71073 \text{ \AA}$) at 50 kV and 40 mA (180 frames, $\Delta\omega=1^\circ$, exposure time per frame: 5 min. The data were corrected by a numerical absorption correction using the program X-Area (Stoe, 2004) as well as for Lorentz and polarisation effects. The structure was solved with direct methods using SHELXS-97³ and refined with full-matrix least-squares on F^2 using the program SHELXL-97⁴ (Sheldrick, 1997). All non-hydrogen atoms were refined anisotropically.

The hydrogen atoms of the methyl group were calculated in their expected positions. The other hydrogen atoms were located from the differences in Fourier map. All hydrogen atoms were refined with $U_{\text{iso}}(\text{H}) = 1.2 U_{\text{eq}}(\text{C,N})$. The unit cell contains channels filled with disordered solvent molecules. In spite of several attempts, no chemically reasonable solution could be received for the solvent species in the channels of the crystal material. Very high displacement parameters, high esdimates and partial occupancy due to the disorder make it impossible to determine accurate atomic positions for that molecules. PLATON/SQUEEZE⁵ calculated a solvent-accessible void volume in the unit cell of 2085.2 \AA^3 (40.8 % of the total cell volume), corresponding to 362 electrons (residual electron density after the last

refinement cycle) per cell. This number agrees with about 0.5 molecules of DMF (0.5x40x18=360) per asymmetric unit. The contributions of the disordered solvent species was subtracted from the structure factor calculations, but included in D(calc), F000 & Mol.Wght. The deposited atom data (cif) reflect on only known cell content.

CCDC 942281 for IFP-5 contains the supplementary crystallographic data for this paper. These data can be obtained free of charge from The Cambridge Crystallographic Data Centre via www.ccdc.cam.ac.uk/data_request/cif.

Table S1. Crystal Data, Details of Intensity Measurements, and Structure Refinement for [Co(L1)] · 0.5 DMF (IFP-5).

| | |
|---|--|
| Empirical formula | C _{7.5} H _{9.5} N _{4.5} O _{2.5} Co |
| Formula weight / g·mol ⁻¹ | 261.63 |
| Crystal system | trigonal |
| Space group | <i>R</i> -3 |
| Cell dimensions <i>a</i> = <i>b</i> / Å <i>c</i> / Å <i>α</i> = <i>β</i> / ° <i>γ</i> / ° | 17.7780(13) 18.6259(13) 90 120 |
| Volume / Å ³ | 5105.6(6) |
| Temperature / K | 210 |
| <i>Z</i> | 18 |
| Density (calculated) / g·cm ⁻³ | 1.53 |
| Absorptions coefficient / cm ⁻¹ | 1.506 |
| Radiation (λ / Å) | MoK _α (0.71073) |
| 2θ range / ° | 3.44 – 49.98 |
| crystal size / mm | 0.16 × 0.13 × 0.11 |
| F(000) | 2394 |
| Index ranges | -21 ≤ <i>h</i> ≤ 21 -21 ≤ <i>k</i> ≤ 21 -22 ≤ <i>l</i> ≤ 22 |
| Reflections collected | 11007 |
| Independend reflections | 2002 (<i>R</i> _{int} =0.0521) |
| Min. and max. transmission | 0.7279 and 0.8078 |
| Data / restraints / parameters | 2002 / 0 / 128 |
| <i>R</i> ₁ / <i>wR</i> ₂ [<i>I</i> > 2σ(<i>I</i>)] | 0.0482 / 0.1142 |
| <i>R</i> ₁ / <i>wR</i> ₂ (all data) | 0.0772 / 0.1245 |
| <i>S</i> on <i>F</i> ² | 0.984 |
| Largest diff. peak and hole / e·Å ⁻³ | 0.766 and -0.359 |

$$w = 1/[\sigma^2(F_o^2) + (0.0715P)^2] \text{ where } P = (F_o^2 + 2F_c^2)/3$$

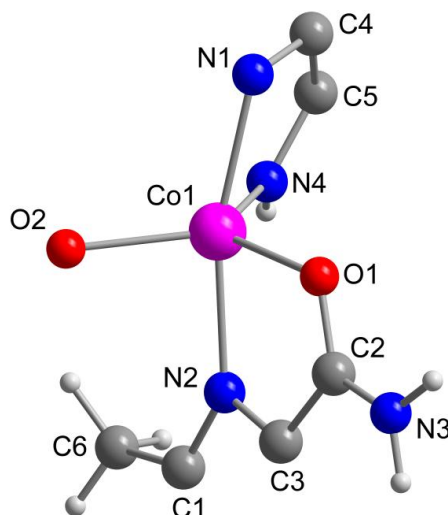


Fig. S9. Asymmetric unit of IFP-5

Table S2. Hydrogen-bonding parameters [\AA , $^\circ$] for $[\text{Co}(\text{L1})] \cdot 0.5 \text{ DMF}$ (IFP-5).

| | D-H | H \cdots A | D \cdots A | D-H \cdots A |
|------------------------------------|---------|--------------|--------------|----------------|
| N3 - H3A \cdots O2 ^{VI} | 0.91(6) | 1.94(6) | 2.800(4) | 157(5) |
| N3 - H3B \cdots O1 ^{IX} | 0.91(6) | 2.17(7) | 3.024(5) | 156(5) |
| N4 - H4 \cdots N1 ^X | 0.81(5) | 2.44(5) | 3.189(5) | 156(5) |

Symmetry operators:

$$\begin{array}{llll}
 \text{I } x-y, x-1, 1-z & \text{II } 4/3-x, -y-1/3, 2/3-z & \text{III } y+1/3, 2/3-x+y, 2/3-z & \text{IV } 2/3+y, 1/3-x+y, 1/3-z \\
 \text{V } 4/3-x+y, 2/3-x, z-1/3 & \text{VI } 1/3+x-y, x-1/3, 2/3-z & \text{VII } 1/3+x-y, x-1/3, 2/3-z & \text{VIII } 1+y, 1-x+y, 1-z \\
 \text{IX } 2/3-y, x-y-2/3, 1/3+z & \text{X } 5/3-x, 1/3-y, 1/3-z & \text{XI } y+2/3, y-x+1/3, 1/3-z & \text{XII } x-y-1/3, x-2/3, 1/3-z \\
 \text{XIII } 1+y, 1-x+y, -z & & &
 \end{array}$$

Thermogravimetric (TG) analysis

The TG measurements were performed in a stationary air atmosphere (no purge) from room temperature up to 800 $^\circ\text{C}$ using a Linseis thermal analyzer (Linseis, Germany) working in the vertical mode. The heating rate was 10 $^\circ\text{C}/\text{min}$. The samples were placed in cups of aluminium oxide.

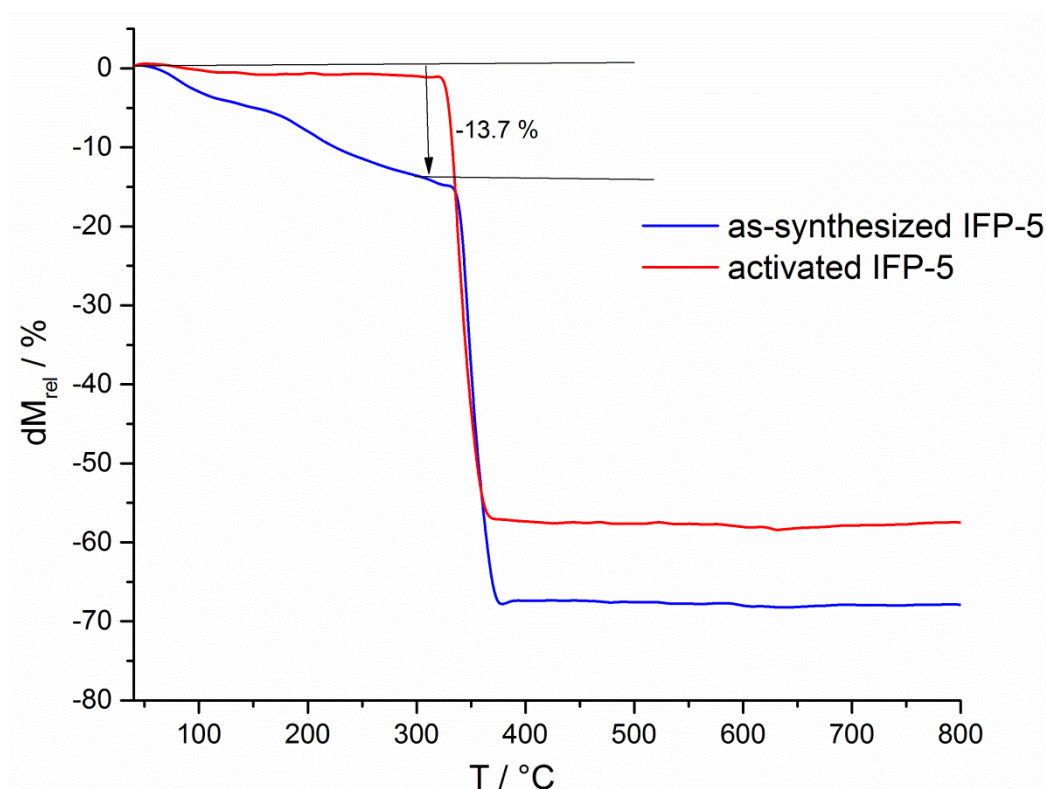


Fig. S10. TGA curves of as-synthesized and activated IFP-5.

Gas-sorption measurements

The sample was connected to the preparation port of the sorption analyzer and degassed under vacuum until the out gassing rate, i.e., the rate of pressure rise in the temporarily closed manifold with the connected sample tube, was less than 2 μ Torr/min at the specified temperature 200 $^{\circ}$ C for 24 h. After weighing, the sample tube was then transferred to the analysis port of the sorption analyzer. All used gases (H_2 , He, N_2 , CO_2 , CH_4) were of ultra high purity (UHP, grade 5.0, 99.999%) and the STP volumes are given according to the NIST standards (293.15 K, 101.325 kPa). Helium gas was used for the determination of the cold and warm free space of the sample tubes. H_2 and N_2 sorption isotherms were measured at 77 K (liquid nitrogen bath), whereas CO_2 and CH_4 sorption isotherms were measured at 298 ± 1 K (passive thermostating) 273.15 K (ice/deionized water bath) and 195.0 K (acetone/dry ice). The heat of adsorption values and the DFT calculations (' N_2 DFT slit pore' model) were done using the ASAP 2020 v3.05 software.

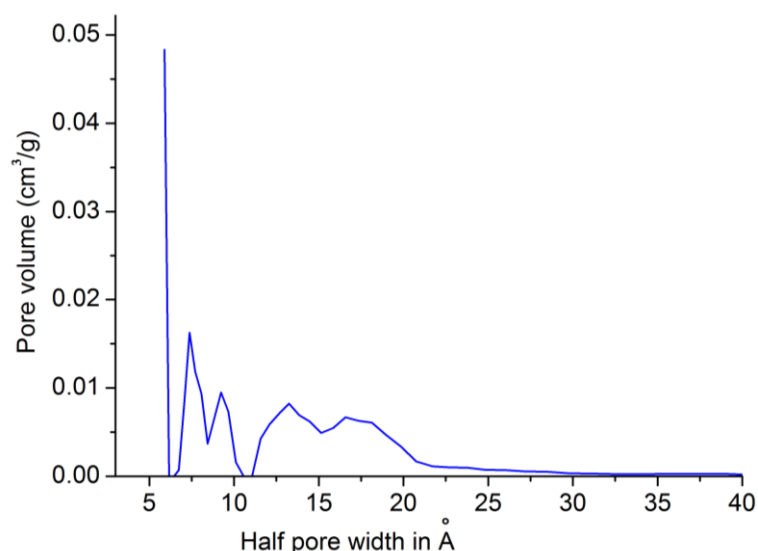


Fig. S11. NL-DFT pore size distribution curve of IFP-5.

Heat of adsorption

From two adsorption isotherms acquired at different temperatures T_1 and T_2 , the differential heat of adsorption $\Delta H_{ads,diff}$ can be calculated for any amount of adsorbed substance after determining the required relative pressures p_1 and p_2 . A modified form of the Clausius-Clapeyron equation is used (eq (1))⁶ $\Delta H_{ads,diff}$ was calculated over the whole adsorption range from the 273 K and 298 K isotherms for CO₂.

$$\Delta H_{ads,diff} = -R \ln \left(\frac{p_2}{p_1} \right) \frac{T_1 T_2}{T_2 - T_1} \quad (1)$$

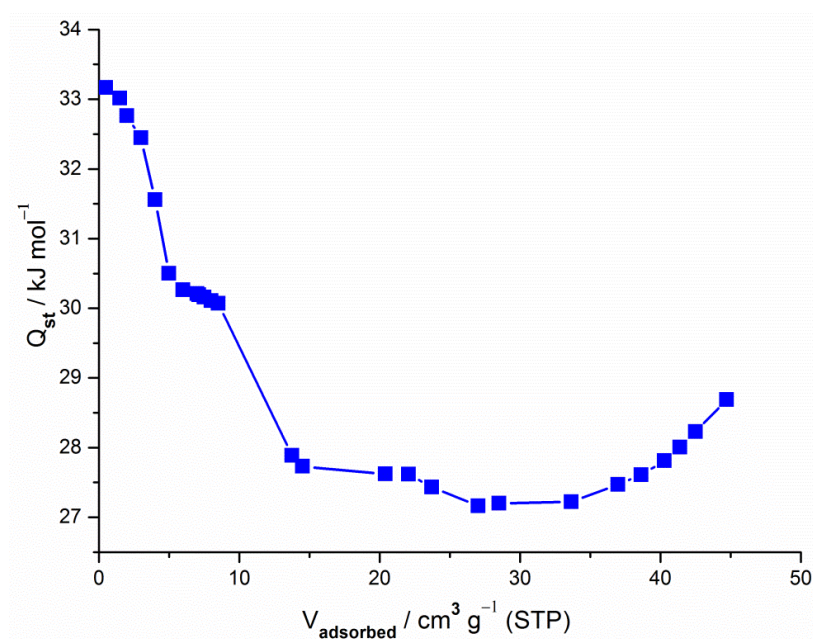


Fig. S12. Isosteric heats of CO₂ adsorption as a function of the adsorbent loading for IFP-5.

Magnetic Measurement

Temperature-dependent magnetic susceptibility measurements were carried out with a *Quantum-Design* MPMS-XL-5 SQUID magnetometer equipped with a 5 Tesla magnet in the range from 295 to 2.0 K at a magnetic field of 0.5 T. The samples were contained in a gel bucket and fixed in a non-magnetic sample holder. Each raw data file for the measured magnetic moment was corrected for the diamagnetic contribution of the sample holder and the gel bucket. The molar susceptibility data were corrected for the diamagnetic contribution.

Field-dependent magnetisation measurements were carried out in the range from 0 to 5 T and 5 to 0 T at a constant temperature of 2 K.

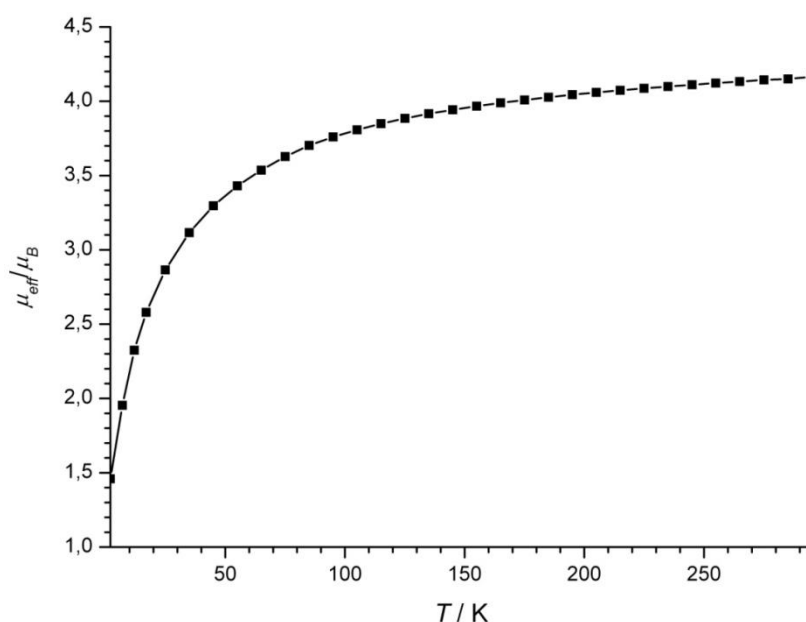


Fig. S13. μ_{eff}/μ_B vs. T curve for IFP-5.

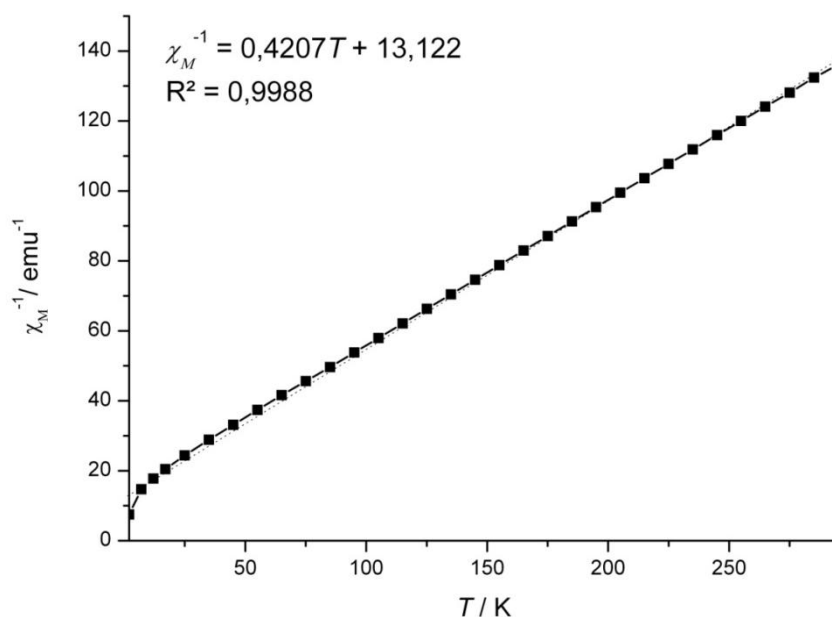


Fig. S14. χ_M^{-1} vs. T curve for IFP-5.

References

1. Yanagisawa, Y. Amemiya, T. Kanazaki, Y. Shimoji, K. Fujimoto, Y. Kitahara, T. Sada, M. Mizuno, M. Ikeda, S. Miyamoto, Y. Furukawa and H. Koike, *J. Med. Chem.*, 1996, **39**, 323.
2. A. R. Katritzky, S. Singh, K. Kirichenko, M. Smiglak, J. D. Holbrey, W. M. Reichert, S. K. Spear and R. D. Rogers, *Chem. Eur. J.*, 2006, **12**, 4630.
3. G. M. Sheldrick, SHELXS-97 Program for the Crystal Structure Solution, University of Göttingen, Germany, 1997.
4. G. M. Sheldrick, SHELXL-97 Program for the Crystal Solution Refinement, University of Göttingen, Germany, 1997.
5. A. L. Spek, *PLATON*, Multipurpose Crystallographic Tool, Utrecht University, Utrecht, The Netherlands, 2008.
6. F. Rouquerol, J. Rouquerol and K. Sing, Adsorption by powders and porous solids, (F. Rouquerol, J. Rouquerol, K. Sing, Eds.), Academic Press, San Diego, 1999, vol. 11